The Optical Gravitational Lensing Experiment. OGLE-III Photometric Maps of the Large Magellanic Cloud[*]

A. U d a l s k i[1], **I. S o s z y ń s k i**[1], **M.K. S z y m a ń s k i**[1], **M. K u b i a k**[1], **G. P i e t r z y ń s k i**[1,2], **Ł. W y r z y k o w s k i**[3,1], **O. S z e w c z y k**[2,1], **K. U l a c z y k**[1] **and R. P o l e s k i**[1]

[1] Warsaw University Observatory, Al. Ujazdowskie 4, 00-478 Warszawa, Poland
e-mail: (udalski,soszynsk,msz,mk,pietrzyn,wyrzykow,szewczyk,kulaczyk,rpoleski)
@astrouw.edu.pl
[2] Universidad de Concepción, Departamento de Fisica, Casilla 160–C, Concepción, Chile
[3] Institute of Astronomy, University of Cambridge, Madingley Road, Cambridge CB3 0HA, UK

ABSTRACT

We present the OGLE-III Photometric Maps of the Large Magellanic Cloud. They cover about 40 square degrees of the LMC and contain mean, calibrated *VI* photometry and astrometry of about 35 million stars observed during seven observing seasons of the third phase of the Optical Gravitational Lensing Experiment – OGLE-III.

We discuss the quality of data and present color–magnitude diagrams of selected fields. The OGLE-III Photometric Maps of the LMC are available to the astronomical community from the OGLE Internet archive.

Magellanic Clouds – Surveys – Catalogs – Techniques: photometric

1 Introduction

One of the important results of the second phase of the Optical Gravitational Lensing Experiment was publication of the OGLE Photometric Maps of Dense Stellar Regions (Udalski *et al.* 1998, 2000, 2002) containing precisely calibrated *BVI* photometry and astrometry of the SMC, LMC and Galactic bulge fields observed during OGLE-II. Because these regions of the sky are extremely interesting from the astrophysical point of view, OGLE maps have been widely used by astronomers worldwide for many astrophysical applications.

OGLE-III phase of the OGLE project, started on June 12, 2001 and still in operation, was a significant extension of the OGLE survey. Much larger observing capabilities made it possible to cover practically entire area of the LMC and SMC and large fraction of the Galactic bulge. After seven years of continuous observations the huge collection of OGLE images was re-reduced to obtain the final precise photometry, calibrated to the standard system (Udalski *et al.* 2008). Thus it became possible to extend the OGLE-II maps to new regions, not observed by OGLE before.

In this paper we present the OGLE-III photometric maps of the Large Magellanic Cloud. They are available to the astronomical community from the OGLE Internet archive.

---

[*] Based on observations obtained with the 1.3 m Warsaw telescope at the Las Campanas Observatory of the Carnegie Institution of Washington.

2 Observations

OGLE-III images of the LMC used for construction of the OGLE-III Photometric Maps of this galaxy were collected between July 2001 and March 2008 and cover seven observing seasons of the LMC. Observations were carried out at Las Campanas Observatory, operated by the Carnegie Institution of Washington, with 1.3 m Warsaw telescope equipped with the eight chip mosaic camera (Udalski 2003). One full mosaic image covers approximately $35' \times 35'$ on the sky with the scale of $0\rlap{.}''26$/pixel.

As the main goal of the OGLE survey is the search for variability of observed objects, the majority of observations were obtained through the single, namely I-band filter. Although this filter well approximates the standard one for $V-I < 3$ mag colors, one has to be aware that for very red objects some deviation may be present. Several hundred I-band images were collected for each of the observed fields. From time to time the LMC fields were also observed in the V-band – typically about 40–50 times in the considered period. The exposure time was set to 180 and 240 seconds in the I and V-band, respectively.

Because the majority of observed fields have high stellar density, observations were conducted only in good seeing and transparency conditions. When the seeing exceeded $1\rlap{.}''8$ observations were stopped. The median seeing of the V and I-band OGLE-III LMC datasets is equal to $1\rlap{.}''2$.

Table 1 lists all LMC fields observed during OGLE-III phase. It also provides equatorial coordinates of their centers and number of stars detected in the I-band. The total observed area reaches 40 square degrees. Fig. 1 presents a combined image of the LMC taken by the ASAS survey program (Pojmański, 1997) with contours of the OGLE-II and OGLE-III fields.

3 Data Reductions

Initial pre-reductions of the collected images – de-biasing, flatfielding – are done at the telescope, immediately after the last pixel of the image is written to the main data acquisition computer (Udalski 2003). Although the first, provisional photometry is done also in almost real time at the telescope, photometry used in this paper comes from the final off-line re-reductions of the entire LMC dataset collected so far. Photometry is based on the Difference Image Analysis method (DIA – Alard and Lupton 1998, Woźniak 2000) and all details on the OGLE-III implementation and calibration to the standard system can be found in Udalski *et al.* (2008). Comparison with the OGLE-II photometric maps indicates that the mean difference of the magnitudes between the calibrated OGLE-III and OGLE-II photometry for about 800000 stars brighter than $I < 18$ mag and $V < 19$ mag in overlaping fields is negligible ($-0.004 \pm 0.013, -0.003 \pm 0.013$ in the I and V, respectively when calibrating directly with standard stars from Landolt's (1992) fields or $0.001 \pm 0.010, 0.000 \pm 0.007$ for final calibrations of OGLE-III photometry with OGLE-II maps) implying that OGLE-II and OGLE-III maps are photometrically fully consistent.

Astrometric transformation of the pixel grid to equatorial system was done in similar way as in the OGLE-II maps. Details can also be found in Udalski *et al.* (2008).

4 Construction of Photometric Maps

Because the OGLE-III photometric databases are constructed separately for I and V-band data, the first step of map preparation was the cross-identification of V-band counterparts to each I-band object. Due to some shifts between respective I and V-band

Table 1

OGLE-III Fields in the LMC

Field	RA (2000)	DEC (2000)	$N_{\rm Stars}$	Field	RA (2000)	DEC (2000)	$N_{\rm Stars}$
LMC100	$5^{\rm h}19^{\rm m}02{.}2$	$-69°15'07''$	1075711	LMC158	$4^{\rm h}30^{\rm m}59{.}9$	$-70°26'01''$	34264
LMC101	$5^{\rm h}19^{\rm m}03{.}1$	$-68°39'19''$	548707	LMC159	$5^{\rm h}25^{\rm m}11{.}4$	$-68°03'58''$	234254
LMC102	$5^{\rm h}19^{\rm m}03{.}4$	$-68°03'48''$	266963	LMC160	$5^{\rm h}25^{\rm m}20{.}9$	$-68°39'24''$	437897
LMC103	$5^{\rm h}19^{\rm m}02{.}9$	$-69°50'26''$	833034	LMC161	$5^{\rm h}25^{\rm m}32{.}5$	$-69°14'59''$	787467
LMC104	$5^{\rm h}19^{\rm m}02{.}4$	$-70°26'03''$	472959	LMC162	$5^{\rm h}25^{\rm m}43{.}3$	$-69°50'24''$	1171172
LMC105	$5^{\rm h}19^{\rm m}01{.}6$	$-71°01'31''$	353469	LMC163	$5^{\rm h}25^{\rm m}52{.}2$	$-70°25'55''$	806912
LMC106	$5^{\rm h}19^{\rm m}01{.}0$	$-71°36'57''$	236384	LMC164	$5^{\rm h}26^{\rm m}08{.}4$	$-71°01'23''$	381352
LMC107	$5^{\rm h}13^{\rm m}01{.}5$	$-66°52'57''$	226287	LMC165	$5^{\rm h}26^{\rm m}20{.}9$	$-71°37'01''$	329028
LMC108	$5^{\rm h}13^{\rm m}01{.}9$	$-67°28'40''$	257801	LMC166	$5^{\rm h}31^{\rm m}20{.}1$	$-68°03'51''$	314715
LMC109	$5^{\rm h}12^{\rm m}53{.}3$	$-68°04'06''$	294145	LMC167	$5^{\rm h}31^{\rm m}39{.}6$	$-68°39'32''$	394585
LMC110	$5^{\rm h}12^{\rm m}43{.}6$	$-68°39'42''$	529605	LMC168	$5^{\rm h}32^{\rm m}01{.}4$	$-69°15'00''$	636559
LMC111	$5^{\rm h}12^{\rm m}32{.}7$	$-69°15'02''$	696121	LMC169	$5^{\rm h}32^{\rm m}22{.}8$	$-69°50'26''$	1092986
LMC112	$5^{\rm h}12^{\rm m}21{.}5$	$-69°50'21''$	752907	LMC170	$5^{\rm h}32^{\rm m}48{.}1$	$-70°25'53''$	878425
LMC113	$5^{\rm h}12^{\rm m}10{.}9$	$-70°25'48''$	561679	LMC171	$5^{\rm h}33^{\rm m}10{.}6$	$-71°01'30''$	513519
LMC114	$5^{\rm h}11^{\rm m}58{.}9$	$-71°01'22''$	221912	LMC172	$5^{\rm h}33^{\rm m}34{.}4$	$-71°36'54''$	423099
LMC115	$5^{\rm h}07^{\rm m}09{.}7$	$-66°52'59''$	234177	LMC173	$5^{\rm h}37^{\rm m}29{.}3$	$-68°03'50''$	221971
LMC116	$5^{\rm h}07^{\rm m}00{.}9$	$-67°28'29''$	205536	LMC174	$5^{\rm h}37^{\rm m}59{.}8$	$-68°39'26''$	340208
LMC117	$5^{\rm h}06^{\rm m}55{.}3$	$-68°03'58''$	527346	LMC175	$5^{\rm h}38^{\rm m}32{.}3$	$-69°15'01''$	497977
LMC118	$5^{\rm h}06^{\rm m}25{.}4$	$-68°39'25''$	694697	LMC176	$5^{\rm h}39^{\rm m}01{.}6$	$-69°50'30''$	576984
LMC119	$5^{\rm h}06^{\rm m}02{.}5$	$-69°15'02''$	817851	LMC177	$5^{\rm h}39^{\rm m}38{.}0$	$-70°25'49''$	817966
LMC120	$5^{\rm h}05^{\rm m}39{.}8$	$-69°50'28''$	617701	LMC178	$5^{\rm h}40^{\rm m}14{.}1$	$-71°01'27''$	471477
LMC121	$5^{\rm h}05^{\rm m}14{.}4$	$-70°25'59''$	442352	LMC179	$5^{\rm h}40^{\rm m}52{.}3$	$-71°36'58''$	296759
LMC122	$5^{\rm h}04^{\rm m}52{.}9$	$-71°01'25''$	288282	LMC180	$5^{\rm h}40^{\rm m}51{.}5$	$-72°12'28''$	258973
LMC123	$5^{\rm h}01^{\rm m}18{.}0$	$-66°53'00''$	242827	LMC181	$5^{\rm h}43^{\rm m}35{.}7$	$-68°03'58''$	201579
LMC124	$5^{\rm h}01^{\rm m}00{.}3$	$-67°28'27''$	290411	LMC182	$5^{\rm h}44^{\rm m}16{.}0$	$-68°39'32''$	311362
LMC125	$5^{\rm h}00^{\rm m}36{.}1$	$-68°03'54''$	357288	LMC183	$5^{\rm h}45^{\rm m}02{.}8$	$-69°14'59''$	361838
LMC126	$5^{\rm h}00^{\rm m}02{.}4$	$-68°39'31''$	530735	LMC184	$5^{\rm h}45^{\rm m}40{.}2$	$-69°50'33''$	486666
LMC127	$4^{\rm h}59^{\rm m}33{.}6$	$-69°14'54''$	547901	LMC185	$5^{\rm h}46^{\rm m}30{.}8$	$-70°25'51''$	630366
LMC128	$4^{\rm h}59^{\rm m}03{.}6$	$-69°50'24''$	406243	LMC186	$5^{\rm h}47^{\rm m}21{.}2$	$-71°01'24''$	376966
LMC129	$4^{\rm h}58^{\rm m}24{.}6$	$-70°26'07''$	304616	LMC187	$5^{\rm h}48^{\rm m}12{.}6$	$-71°36'52''$	298070
LMC130	$4^{\rm h}57^{\rm m}50{.}8$	$-71°01'20''$	231039	LMC188	$5^{\rm h}48^{\rm m}26{.}6$	$-72°12'27''$	152482
LMC131	$4^{\rm h}55^{\rm m}28{.}6$	$-66°52'46''$	248421	LMC189	$5^{\rm h}50^{\rm m}37{.}9$	$-68°39'26''$	153656
LMC132	$4^{\rm h}55^{\rm m}00{.}6$	$-67°28'36''$	217827	LMC190	$5^{\rm h}51^{\rm m}33{.}2$	$-69°14'55''$	200564
LMC133	$4^{\rm h}54^{\rm m}29{.}2$	$-68°03'47''$	346558	LMC191	$5^{\rm h}52^{\rm m}20{.}1$	$-69°50'24''$	243558
LMC134	$4^{\rm h}53^{\rm m}49{.}2$	$-68°39'18''$	304271	LMC192	$5^{\rm h}53^{\rm m}24{.}1$	$-70°25'51''$	228516
LMC135	$4^{\rm h}53^{\rm m}05{.}2$	$-69°14'51''$	284846	LMC193	$5^{\rm h}54^{\rm m}21{.}7$	$-71°01'34''$	138223
LMC136	$4^{\rm h}52^{\rm m}23{.}7$	$-69°50'25''$	244490	LMC194	$5^{\rm h}55^{\rm m}29{.}7$	$-71°36'59''$	77816
LMC137	$4^{\rm h}51^{\rm m}30{.}2$	$-70°26'01''$	200058	LMC195	$5^{\rm h}56^{\rm m}00{.}0$	$-72°12'25''$	43002
LMC138	$4^{\rm h}49^{\rm m}34{.}7$	$-66°53'07''$	117664	LMC196	$5^{\rm h}56^{\rm m}54{.}7$	$-68°39'29''$	116258
LMC139	$4^{\rm h}49^{\rm m}05{.}2$	$-67°28'30''$	128858	LMC197	$5^{\rm h}58^{\rm m}02{.}7$	$-69°15'06''$	92295
LMC140	$4^{\rm h}48^{\rm m}18{.}2$	$-68°04'05''$	188164	LMC198	$5^{\rm h}59^{\rm m}02{.}5$	$-69°50'35''$	71992
LMC141	$4^{\rm h}47^{\rm m}26{.}7$	$-68°39'36''$	191197	LMC199	$6^{\rm h}00^{\rm m}14{.}7$	$-70°26'00''$	63841
LMC142	$4^{\rm h}46^{\rm m}31{.}9$	$-69°15'08''$	225807	LMC200	$6^{\rm h}01^{\rm m}27{.}5$	$-71°01'36''$	58765
LMC143	$4^{\rm h}45^{\rm m}43{.}1$	$-69°50'19''$	155672	LMC201	$6^{\rm h}02^{\rm m}45{.}9$	$-71°37'04''$	91051
LMC144	$4^{\rm h}44^{\rm m}40{.}2$	$-70°26'01''$	116363	LMC202	$6^{\rm h}03^{\rm m}28{.}3$	$-72°12'34''$	79469
LMC145	$4^{\rm h}43^{\rm m}47{.}5$	$-66°52'43''$	64628	LMC203	$6^{\rm h}03^{\rm m}29{.}9$	$-72°48'04''$	71396
LMC146	$4^{\rm h}43^{\rm m}03{.}0$	$-67°28'17''$	86656	LMC204	$6^{\rm h}03^{\rm m}14{.}6$	$-68°39'25''$	108173
LMC147	$4^{\rm h}42^{\rm m}07{.}8$	$-68°03'55''$	103604	LMC205	$6^{\rm h}04^{\rm m}32{.}9$	$-69°15'04''$	82072
LMC148	$4^{\rm h}41^{\rm m}06{.}8$	$-68°39'27''$	110885	LMC206	$6^{\rm h}05^{\rm m}40{.}3$	$-69°50'27''$	78179
LMC149	$4^{\rm h}40^{\rm m}05{.}1$	$-69°14'57''$	115117	LMC207	$6^{\rm h}07^{\rm m}04{.}2$	$-70°25'55''$	70889
LMC150	$4^{\rm h}39^{\rm m}05{.}3$	$-69°50'16''$	96039	LMC208	$6^{\rm h}08^{\rm m}30{.}4$	$-71°01'27''$	87619
LMC151	$4^{\rm h}37^{\rm m}51{.}6$	$-70°25'45''$	89935	LMC209	$6^{\rm h}10^{\rm m}07{.}0$	$-71°37'00''$	64885
LMC152	$4^{\rm h}37^{\rm m}54{.}1$	$-66°52'52''$	46107	LMC210	$6^{\rm h}10^{\rm m}55{.}7$	$-72°12'37''$	70282
LMC153	$4^{\rm h}37^{\rm m}01{.}7$	$-67°28'30''$	56016	LMC211	$6^{\rm h}11^{\rm m}22{.}0$	$-72°48'04''$	61205
LMC154	$4^{\rm h}35^{\rm m}59{.}1$	$-68°04'02''$	65095	LMC212	$6^{\rm h}11^{\rm m}04{.}0$	$-69°14'50''$	81878
LMC155	$4^{\rm h}34^{\rm m}49{.}4$	$-68°39'32''$	71173	LMC213	$6^{\rm h}12^{\rm m}17{.}9$	$-69°50'37''$	52207
LMC156	$4^{\rm h}33^{\rm m}32{.}7$	$-69°15'00''$	72805	LMC214	$6^{\rm h}13^{\rm m}58{.}2$	$-70°26'08''$	60410
LMC157	$4^{\rm h}32^{\rm m}23{.}8$	$-69°50'26''$	44165	LMC215	$6^{\rm h}15^{\rm m}36{.}4$	$-71°01'28''$	60801

reference images of a given subfield and larger than single detector dimensions size of the reference images to mask the gaps between chips of the OGLE-III mosaic camera, the *V*-band counterparts of objects located close to the border in the *I*-band reference image may be present in more than one field. Therefore in the first step third order transformation between pixel grids of a given *I*-band subfield reference image and all *V*-band reference images of subfields that even partially overlap were derived. Then for all *I*-band database objects of a given subfield their corresponding *V*-band counterparts in all fields were found.

The mean photometry was derived for all objects with minimum of 4 and 6 observations in the *V* and *I*-band, respectively, by averaging all observations after removing 5σ deviating points. In the case of multiple *V*-band cross-identifications all *V*-band observations formed a single dataset and then were averaged because they are independent measurements. Finally, the color term correction was applied for each object to its database average magnitude according to the transformation equations and color term coefficients presented in Udalski *et al.* (2008). After the transformation of the $V - I$ color to the standard system, *I* and *V* magnitudes were appropriately adjusted. For objects that do not have color information the average color of the LMC population $V - I = 0.7$ mag was used for color correction of respective *I* or *V* magnitude.

Table 2 presents the first 25 entries from the map of the LMC100.1 subfield. The columns contain: (1) ID number; (2,3) equatorial coordinates J2000.0; (4,5) X, Y pixel coordinates in the *I*-band reference image; (6,7,8) photometry: V, $V - I$, I; (9,10,11) number of points for average magnitude in *V*, number of 5σ removed points in *V*, σ of magnitude for *V*-band; (12,13,14) same as (9,10,11) for the *I*-band. 9.999 or 99.999 markers mean "no data". -1 in column (10) indicates multiple *V*-band cross-identification (the average magnitude and standard deviation are calculated for merged photometry).

The full set of the OGLE-III Photometric Maps is available from the OGLE Internet archive (see below).

5 Discussion

OGLE-III Photometric Maps form a significant extension of the OGLE-II maps that covered only central regions of the LMC (*cf.* Fig. 1). The new maps include practically entire area of the LMC and can be used for many projects studying the global structure of this galaxy. Precise, well calibrated *VI* photometry and astrometry makes this dataset a unique tool for many astrophysical applications.

To show the accuracy of the OGLE-III Photometric Maps Figs. 2 and 3 present standard deviation of magnitudes as a function of magnitude in the *V* and *I*-band for two LMC fields: LMC100.1 – very dense field located in the central bar and LMC209.1 – sparsely populated field form the outer parts of this galaxy. As one can expect the accuracy of photometry depends on the stellar density and, for example, $\sigma = 0.1$ mag photometry scatter is reached for stars by about 0.3 magnitude brighter in the densest bar fields than in the uncrowded fields.

Figs. 4 and 5 show the histograms of objects in the *V* and *I*-band for the same two fields. One can notice that the completeness of the maps is high and reaches $V \approx 20.5-21$ mag and $I \approx 20-20.5$ mag. Again, as one can expected, completeness is a function of stellar crowding.
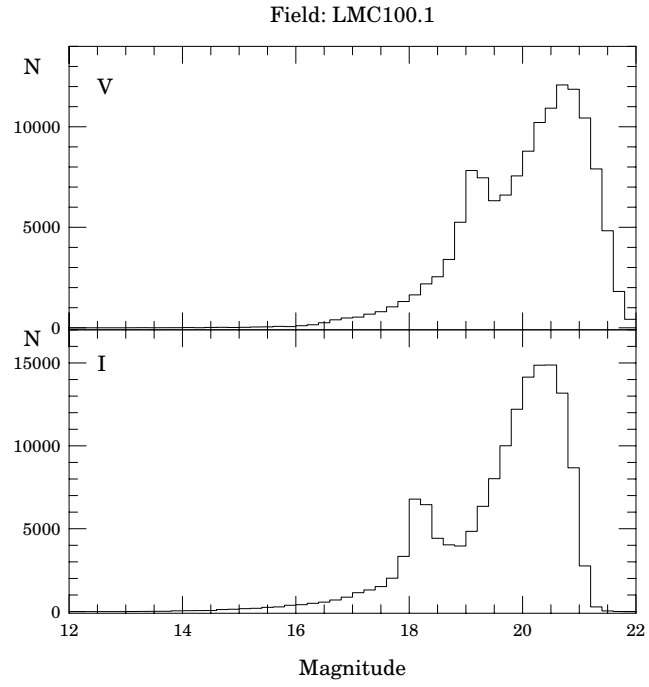
Field: LMC100.1

Fig. 4. Histogram of magnitudes for the central bar subfield LMC100.1.
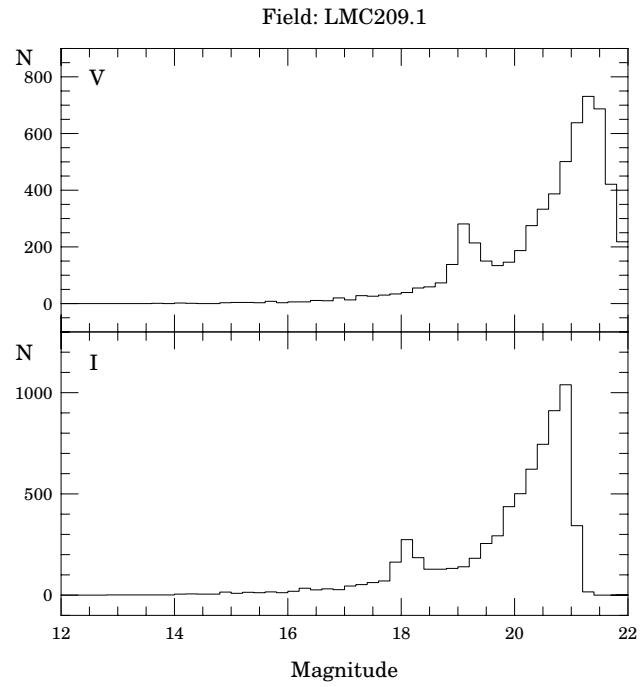
Field: LMC209.1

Fig. 5. Same as in Fig. 5 for the outer subfield LMC209.1.

Table 2

OGLE-III Photometric Map of the LMC100.1 subfield.

ID	RA (2000)	DEC (2000)	X	Y	V	$V-I$	I	N_V	N_V^{bad}	σ_V	N_I	N_I^{bad}	σ_I
1	$5^h19^m05\!\!.^{\!s}97$	$-69°33'17\!\!.''4$	57.08	56.26	16.647	2.483	14.164	35	0	0.127	6	0	0.058
2	$5^h19^m08\!\!.^{\!s}62$	$-69°32'15\!\!.''3$	296.00	110.54	16.331	1.922	14.409	67	-1	0.208	399	0	0.077
3	$5^h19^m08\!\!.^{\!s}67$	$-69°30'56\!\!.''1$	600.20	112.84	17.715	3.062	14.652	47	0	0.157	399	0	0.065
4	$5^h19^m09\!\!.^{\!s}13$	$-69°30'39\!\!.''7$	663.16	122.23	16.318	1.847	14.471	48	0	0.018	402	0	0.010
5	$5^h19^m10\!\!.^{\!s}04$	$-69°29'46\!\!.''7$	866.65	141.47	14.495	0.354	14.141	48	0	0.005	402	0	0.007
6	$5^h19^m11\!\!.^{\!s}95$	$-69°32'00\!\!.''9$	351.08	177.73	17.470	3.182	14.288	44	0	0.680	404	0	0.214
7	$5^h19^m13\!\!.^{\!s}76$	$-69°30'00\!\!.''3$	814.39	216.32	16.530	2.092	14.438	48	0	0.029	404	0	0.015
8	$5^h19^m14\!\!.^{\!s}12$	$-69°29'03\!\!.''2$	1033.50	224.43	14.141	0.188	13.953	48	0	0.004	404	0	0.006
9	$5^h19^m14\!\!.^{\!s}53$	$-69°32'48\!\!.''2$	168.82	228.84	16.917	2.326	14.591	87	-1	0.072	385	0	0.033
10	$5^h19^m16\!\!.^{\!s}07$	$-69°30'03\!\!.''1$	803.47	262.79	14.739	0.780	13.959	48	0	0.005	404	0	0.005
11	$5^h19^m17\!\!.^{\!s}31$	$-69°31'47\!\!.''3$	402.93	285.85	15.366	1.367	13.998	48	0	0.006	404	0	0.005
12	$5^h19^m17\!\!.^{\!s}46$	$-69°29'50\!\!.''9$	850.10	290.92	16.813	2.172	14.641	48	0	0.072	404	0	0.031
13	$5^h19^m19\!\!.^{\!s}14$	$-69°30'12\!\!.''7$	766.32	324.45	17.416	3.007	14.408	47	0	0.286	404	0	0.189
14	$5^h19^m19\!\!.^{\!s}61$	$-69°32'51\!\!.''7$	155.22	330.93	16.432	2.245	14.187	84	-1	0.048	366	0	0.021
15	$5^h19^m19\!\!.^{\!s}54$	$-69°31'44\!\!.''6$	413.08	330.83	16.979	2.371	14.608	48	0	0.131	404	0	0.062
16	$5^h19^m23\!\!.^{\!s}42$	$-69°33'20\!\!.''3$	44.83	407.14	16.310	9.999	99.999	40	0	0.052	0	0	9.999
17	$5^h19^m25\!\!.^{\!s}72$	$-69°29'44\!\!.''3$	874.65	457.67	15.044	1.200	13.844	48	0	0.006	404	0	0.004
18	$5^h19^m27\!\!.^{\!s}42$	$-69°31'18\!\!.''7$	511.94	489.95	15.476	1.214	14.262	48	0	0.008	404	0	0.005
19	$5^h19^m27\!\!.^{\!s}78$	$-69°30'30\!\!.''2$	698.01	498.27	14.010	9.999	99.999	48	0	0.153	0	0	9.999
20	$5^h19^m29\!\!.^{\!s}18$	$-69°30'57\!\!.''9$	591.71	525.78	13.920	-0.135	14.055	48	0	0.006	404	0	0.008
21	$5^h19^m32\!\!.^{\!s}47$	$-69°30'34\!\!.''9$	679.44	592.49	15.383	9.999	99.999	48	0	0.061	0	0	9.999
22	$5^h19^m32\!\!.^{\!s}64$	$-69°30'32\!\!.''9$	687.26	596.09	16.676	9.999	99.999	48	0	0.026	0	0	9.999
23	$5^h19^m33\!\!.^{\!s}45$	$-69°30'18\!\!.''0$	744.46	612.71	14.765	1.573	13.192	48	0	0.008	404	0	0.006
24	$5^h19^m33\!\!.^{\!s}84$	$-69°30'18\!\!.''0$	744.28	620.53	14.906	1.322	13.584	48	0	0.008	404	0	0.007
25	$5^h19^m37\!\!.^{\!s}93$	$-69°31'46\!\!.''7$	402.99	700.88	15.501	2.142	13.359	48	0	0.046	404	0	0.017

Figs. 6–9 show several color–magnitude diagrams (CMDs) constructed directly from the OGLE-III maps. They include CMD of one of the densest central fields of the LMC: LMC100.1, high extinction region near the Tarantula nebula: LMC175.6, as well as regions in the outskirts of this galaxy (LMC121.1 in the western wing and LMC186.1 in the eastern wing). Figs. 6–9 clearly illustrate the quality of data and reveal in details the characteristic features of the LMC stellar populations, as well as show how interstellar extinction affects the CMDs.

6   Data Availability

The OGLE-III Photometric Maps of the LMC are available to the astronomical community from the OGLE Internet Archive:

http://ogle.astrouw.edu.pl   *ftp://ftp.astrouw.edu.pl/ogle3/maps/lmc/*

Beside tables with photometric data and astrometry for each of the subfields the *I*-band reference images are also included. Usage of the data is fully allowed, requiring only the proper acknowledgment to the OGLE project.

REFERENCES

Alard, C., and Lupton, R. 1998, *Astrophys. J.*, **503**, 325.

Landolt, A.U. 1992, *Astron. J.*, **104**, 372.

Pojmański, G. 1997, *Acta Astron.*, **47**, 467.

Udalski, A. 2003, *Acta Astron.*, **53**, 291.

Udalski, A., Szymański, M., Kubiak, M., Pietrzyński, G., Woźniak, P., and Żebruń, K. 1998, *Acta Astron.*, **48**, 147.

Udalski, A., Szymański, M., Kubiak, M., Pietrzyński, G., Soszyński, I., Woźniak, P., and Żebruń, K. 2000, *Acta Astron.*, **50**, 307.

Udalski, A., Szymański, M., Kubiak, M., Pietrzyński, G., Soszyński, I., Woźniak, P., Żebruń, K., Szewczyk, O., and Wyrzykowski, Ł. 2000, *Acta Astron.*, **52**, 217.

Udalski, A., Szymański, M.K., Soszyński, I., and Poleski, R. 2008, *Acta Astron.*, **58**, 69.

Woźniak, P.R. 2000, *Acta Astron.*, **50**, 421.

Captions of JPEG figures.

Fig. 1. OGLE-III fields in the LMC (black squares: 100–215) overplotted on the image obtained by the ASAS all sky survey. Red strips (1–21) mark OGLE-II fields.

Fig. 2. Standard deviation of magnitudes as a function of magnitude for the central bar subfield LMC100.1.

Fig. 3. Same as in Fig. 2 for the outer subfield LMC209.1

Fig. 6. Color–magnitude diagram for the central bar subfield LMC100.1.

Fig. 7. Color–magnitude diagram for the variable extinction subfield LMC175.6.

Fig. 8. Color–magnitude diagram for the western wing subfield LMC121.1

Fig. 9. Color–magnitude diagram for the eastern wing subfield LMC186.1

This figure "fig1.jpg" is available in "jpg" format from:

http://arXiv.org/ps/0807.3889v1

This figure "fig2.jpg" is available in "jpg" format from:

http://arXiv.org/ps/0807.3889v1

This figure "fig3.jpg" is available in "jpg" format from:

http://arXiv.org/ps/0807.3889v1

This figure "fig6.jpg" is available in "jpg" format from:

http://arXiv.org/ps/0807.3889v1

This figure "fig7.jpg" is available in "jpg" format from:

http://arXiv.org/ps/0807.3889v1

This figure "fig8.jpg" is available in "jpg" format from:

http://arXiv.org/ps/0807.3889v1

This figure "fig9.jpg" is available in "jpg" format from:

http://arXiv.org/ps/0807.3889v1